

# Residual Stress Analysis of Cold-Sprayed Copper Coatings by Numerical Simulation

Wenya Li, Kang Yang, Dongdong Zhang, and Xianglin Zhou

(Submitted April 27, 2015; in revised form July 23, 2015)

**In this paper, an analysis on the residual stress evolution of cold-sprayed copper coatings on Cu and Al substrates was performed. To investigate the influences of particle velocity, temperature and material combination on the final residual stresses, an integrated frame of calculation was proposed based on the simulation results obtained from the developed thermo-mechanically coupled Eulerian model. In a single Cu splat, generally speaking, the maximum residual stress and plastic deformation are concentrated at the outside contact zone rather than at the center point of initial impact. The action of friction shear between the particle and substrate during impacting should be considered as one of the essential factors on the final residual stress. And the states of residual stresses can vary significantly depending on the material combination, particle velocity, and temperature. In a single pass Cu coating, the residual stress fluctuates across the coating and there exists both compressive stress and tensile stress within the coating. At a certain range of impacting velocities, the resultant residual stresses increase with the increase of particle velocity. The present simulated results are related to the reported experiments by others, showing that the residual stress states and stress change trend are different from some of the reported results.**

**Keywords** cold spraying, copper coating, numerical simulation, residual stress

## 1. Introduction

In cold spraying, metallic or dielectric substrates are exposed to a high-velocity (300–1200 m/s) jet of small metallic particles accelerated by a supersonic jet of compressed gas at a temperature lower than the melting point of the spray material. Beyond a critical velocity defined by the material properties and process conditions, metallic or metallurgical bonding is obtained (Ref 1–3). Consequently, the deleterious effects of oxidation, phase transformation, decomposition, grain growth, and other problems inherent in the conventional thermal spraying can be minimized or eliminated (Ref 1, 4).

Cold spraying is applied for the surface enhancement of metals to improve their properties such as wear and corrosion resistance, electrical/thermal conductivity (Ref 5). In

all applications, coating integrity is very important, and may be dependent significantly on the quality of bonding between particles within the coating, and that between the coating and the substrate. Residual stress is among the most important factors affecting coating integrity that is closely linked to the properties and service lifetime of materials and components (Ref 6). In the case of thermal sprayed coatings, residual stresses have been confirmed to often lead to peeling and/or delamination of coatings (Ref 4, 7).

Up to now, there are a limited amount of data detailing the residual stresses in cold-sprayed materials whether inside a single-deformed particle or the whole coating (Ref 4–6, 8), though there have been several investigations on residual stress of thermal sprayed coatings (Ref 7, 9). In conventional thermal spraying, the final residual stress profiles are the resultants from deposition stress and thermal stress. The deposition stress is the combined effect of quenching and peening. There are many factors that influence the residual stresses, for example, the temperature difference before and after the impact of a particle upon the substrate, the temperature difference of the substrate-coating system during and after the spraying, and the ability of the substrate and coating to plastically deform and work harden upon impact of the particle. The temperature drop during the solidification of molten particles upon impacting on the substrate leads to tensile stress (as known as quenching stress), because the contraction is restricted by the adhesion to the substrate (Ref 10). The peening stress is a compressive component induced by the high-velocity impact of particles causing plastic deformation of the substrate and/or previously deposited coating. Cooling down after deposition at elevated temperatures, gives rise to thermal stress, due to the difference in coefficients of thermal expansion (CTE) between the coating and substrate (Ref 10).

This article is an invited paper selected from presentations at the 2015 International Thermal Spray Conference, held May 11–14, 2015, in Long Beach, California, USA, and has been expanded from the original presentation.

**Wenya Li, Kang Yang, and Dongdong Zhang**, State Key Laboratory of Solidification Processing, Shaanxi Key Laboratory of Friction Welding Technologies, School of Materials Science and Engineering, Northwestern Polytechnical University, Xi'an 710072, Shaanxi, People's Republic of China; and **Xianglin Zhou**, State Key Laboratory for Advanced Metals and Materials, University of Science and Technology Beijing, Beijing 100083, People's Republic of China. Contact e-mail: liwy@nwpu.edu.cn.

Generally speaking, the final residual stress distribution in cold spraying may be a combined effect of peening stress and thermal stress because the quenching stress is negligible for its relatively low temperature, while in the Ref 10 the authors took quenching stress as one of the factors affecting the final residual stress. In Ref 11, it is considered that the spray operations at substrate temperatures above 400 °C magnify the differential thermal contraction stresses. If the deposition temperatures are above 400 °C, the thermal stress should be considered in cold spraying. But if the temperature is lower than 400 °C, almost no quenching and thermal stress in CS can be present, while only peening stress exists in the coating.

Experimental and numerical methods have been used to study the residual stresses in cold-sprayed coatings. There are some experimental methods including x-ray diffraction (including micro-diffraction), neutron diffraction, ex-situ and in situ curvature measurement, hole-drilling, and layer removal methods (Ref 12). Luzin et al. (Ref 5) used neutron diffraction and Tsui and Clyne's (Ref 13) progressive coating deposition model to study the residual stress profiles in the cold-sprayed Cu and Al coatings, and found that the residual stress state of the coatings depends mainly on the deformation behavior, properties of the coating materials, and the kinetic parameters of the cold spraying process. Suhonen et al. (Ref 10) used an in situ measurement and calculating method [Brenner and Senderoff's equation (Ref 14)] to study the effects of substrate material and substrate pretreatment, to find that the residual stresses are mainly dependent on the substrate/coating material combination, and the surface preparation prior to spraying also has an effect on the final stress of the coating. Ghelichi et al. (Ref 3, 6) investigated the residual stress and fatigue behavior of Al and Al alloy coatings. Their results showed that compressive residual stress could be observed in all the coated sets. Matejcek et al. (Ref 15) argued that although the particle velocity has a profound effect on deposition efficiency, the residual stress value is dependent on the elasto-plastic properties of the particle and substrate rather than the spraying parameters in cold-sprayed Cu coatings, and this conclusion is quite different from others. Rech et al. (Ref 16) investigated the residual stress in cold-sprayed Al coating on an Al6061 alloy substrate using Almen gage method, modified layer removal method, and XRD simultaneously. The presence of tensile stress peaks at interfaces between sequential passes was revealed.

There are always difficulties or limitations when measuring residual stresses and it often takes significant time to accurately measure the residual stress whether inside a single splat or in the entire coating. To reduce the time and effect, numerical simulations have been developed (Ref 4). In this study, to investigate the influences of particle velocity, temperature, and material combination on residual stress in cold-sprayed coatings, numerical simulations were used to study the residual stress in cold-sprayed Cu coatings on Cu and Al substrates (including single splat and single pass coating). Finally, the simulation results are compared with the experimental results reported in the literature.

## 2. Model Description

### 2.1 Single Splat

The residual stresses of Cu particle on Cu or Al substrates were simulated using the commercial software ABAQUS. The Eulerian formulation available in Version 6.13 was used and the multi-material option was selected. As a first approximation, the heat generation from plastic deformation and the heat conduction within the bulk were taken into account. Owing to the axisymmetric characteristic of normal impact, a symmetric model was used as shown in Fig. 1(a). In the simulations, the width and the height of the substrate were five times larger than the particle diameter (20  $\mu\text{m}$ ) to reduce the number of elements and calculation time. The 3D 8-node brick temperature-displacement element EC3D8RT was used in meshing, and just one element in the Z-direction of a size identical to the meshing size. The basic meshing size was 0.2  $\mu\text{m}$  (a meshing resolution: 1/100 dp) as shown in Fig. 1(b). The degrees of freedom in Z-direction were constrained for all elements. Boundary F-G-H was constrained in X-displacement. Boundaries H-I and I-J were fixed (constrained in Y- and X-displacements).

The impact behavior of cold-sprayed Cu particles has been studied using the developed Eulerian model in the previous study (Ref 17, 18). As for the Eulerian method, the overall mesh can be considered as two overlapping meshes, consisting of a background spatial mesh, which is fixed in space, and material, which can flow through the fixed mesh. Therefore, it can avoid the extreme distortion of elements, and the Eulerian formulation on the impacting behavior is necessary due to the clearly extensive plastic deformation involved in CS. Normally it takes about 30 to 40 ns for a Cu particle finishing the impacting process, thus, 1000 ns was set as the solution time in this study to obtain the residual stresses.

### 2.2 Single Pass Coating

The residual stress of single pass Cu particles on Cu or Al substrates was also simulated using a model similar to the one used in single splat in section 2.1. As shown in Fig. 2(a), a cross section from the single pass was taken as the computational domain and the sizes of Cu or Al substrates were  $30 \times 3 \text{ mm}^2$ . As for the Cu particles, a size range from 5 to 50  $\mu\text{m}$  following the modified Rosin-Rammler model (Ref 19) was adopted and had a spatial distribution of 3 mm as shown in Fig. 2(b). In this model, the basic meshing size near the impact zone was 1.5  $\mu\text{m}$  and the thickness in the Z-direction was also 1.5  $\mu\text{m}$ . The solution time in this calculation was 2000 ns.

### 2.3 Material Model

**2.3.1 Material Property and Other Parameters Settings.** For particles and substrates, the material deformation is described by the Johnson and Cook plasticity model, which accounts for strain hardening, strain rate hardening, and thermal softening effects. The yield stress ( $\sigma_y$ ) of this material is expressed as follows (Ref 19, 20):

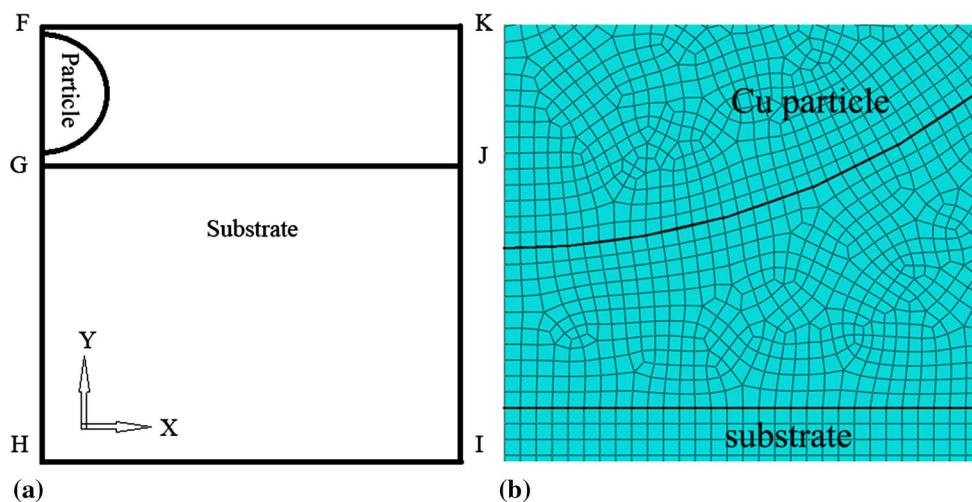


**Fig. 1** (a) Symmetric model and computational domain of Cu particle (20  $\mu\text{m}$ ) impacting on Cu and Al substrates under the Eulerian frame and (b) the enlarged view of elements around the particle with a meshing resolution of 1/100 dp. Note that void material was used for other region

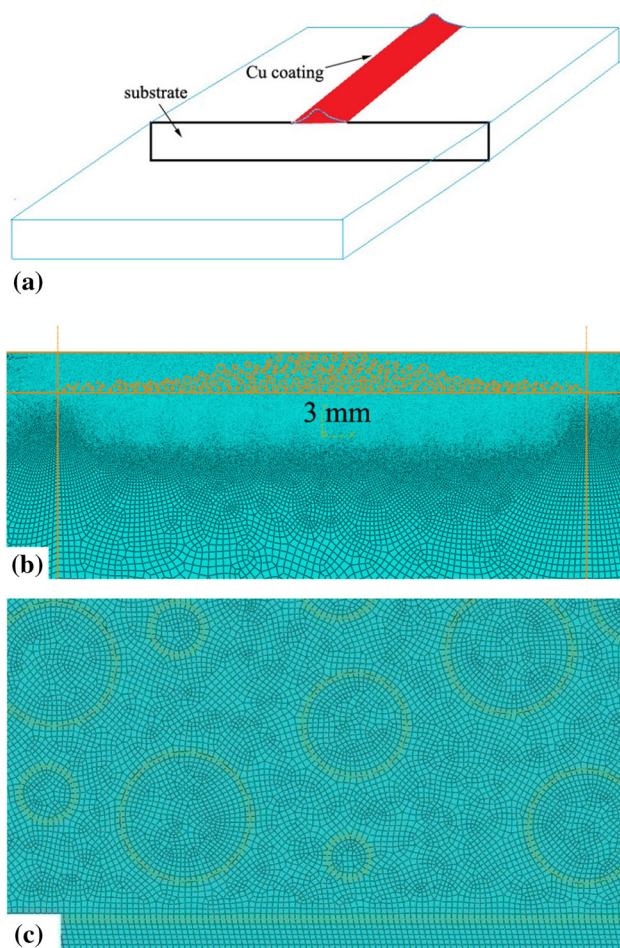


**Fig. 2** (a) Sketch of the single pass model, (b) the meshing and particle arrangement, and (c) the enlarged view of particle meshing

$$\sigma_y = (A + B\epsilon_{\text{eff}}^p)^N (1 + C \ln \dot{\epsilon}^*) (1 - T^{*M}), \quad (\text{Eq 1})$$

where  $A$ ,  $B$ ,  $N$ ,  $C$ ,  $M$  are the constants dependent on materials.  $\epsilon_{\text{eff}}^p$  is the effective plastic strain.  $\dot{\epsilon}^*$  is the effective plastic strain rate normalized with respect to a reference strain rate.  $T^*$  is a homologous temperature defined as the following (Ref 18, 19):

$$T^* = \frac{T - T_{\text{room}}}{T_m - T_{\text{room}}}, \quad (\text{Eq 2})$$

where  $T_m$  is the melting temperature and  $T_{\text{room}}$  is the reference temperature (normally room temperature).

A linear Mie-Gruneisen equation of state (EOS) was employed for the elastic behavior (Ref 17, 18). The linear Us-Up Hugoniot form is defined as (Ref 21)

$$p = \frac{\rho_0 C_0^2 \eta}{(1 - S\eta)^2} \left(1 - \frac{\Gamma_0}{2} \eta\right) + \Gamma_0 \rho_0 E_m, \quad (\text{Eq 3})$$

where  $\eta = 1 - \rho/\rho_0$  is the nominal volumetric compressive strain,  $\rho_0$  the initial density,  $\rho$  the current density,  $C_0$  the bulk speed of sound,  $\Gamma_0$  the material constant named Gruneisen's gamma,  $S$  the linear Hugoniot slope coefficient,  $E_m$  the internal energy per unit reference specific volume.

The mechanical and thermal properties are assumed to be isotropic. The properties used for Cu and Al in the simulations are shown in Table 1 (Ref 17). It was assumed that the initial temperatures of particle and substrate are 25  $^\circ\text{C}$ .

**2.3.2 Governing Equation.** The conservation equations in the Eulerian description are written using the spatial time derivative. The mass, momentum, and energy equations are (Ref 22)

$$\frac{d\rho}{dt} = -\rho \frac{\partial u}{\partial x} \quad (\text{Eq 4})$$

$$\frac{dE}{dt} = \frac{1}{\rho} \sigma_{ij} \frac{\partial u}{\partial x} \quad (\text{Eq } 5)$$

$$\frac{du}{dt} = \frac{1}{\rho} \frac{\partial \sigma_y}{\partial x}, \quad (\text{Eq } 6)$$

where  $\rho$  is the density,  $\sigma$  the Cauchy stress,  $u$  the material velocity, and  $E$  the total energy per unit volume. The total energy  $E$  is the sum of the kinetic energy and the internal energy  $e$ , which is

$$E = \frac{1}{2} \rho u \cdot u + e. \quad (\text{Eq } 7)$$

### 3. Results and Discussion

#### 3.1 Residual Stress in a Single Splat

**3.1.1 The Influence of Particle Velocity.** Figure 3 and 4 show the simulation results of the Cu material volume fraction (EVF) in elements, the effective plastic strain (PEEQ), and the residual stresses (including impacting particle and substrate) after impacting at velocities of 500, 600, and 700 m/s as reported in Ref 15. It is found that the narrow interfacial region experienced intensive deformation and a crater was developed in the flat substrate. Moreover, the maximum plastic deformation is concentrated at the surrounding of the contact zone rather than the center point of initial impact as reported in Ref 17. The zone of high strain is extruded in a plasticized state to form a jet and the jet gets elongated with the increase of impacting velocity as shown in Fig. 3 and 4.

In the simulation of Cu/Cu, corresponding to the PEEQ distribution, the residual stress at the surrounding area of the contact zone is larger than that of the center area. The residual stress in other areas inside the impacting particle is small, which is a typical feature of cold spraying (Ref 15). The impacting particle has deformed more extensively with increasing velocity from 500

**Table 1** Properties of the used Cu in this study

| Material                               | Cu    | Al    |
|--|-------|-------|
| Density, kg/m <sup>3</sup>             | 8960  | 2700  |
| Heat capacity, J/(kg K)                | 383   | 880   |
| Thermal conductivity, W/(m K)          | 386   | 237   |
| Young's modulus, GPa                   | 124   | 69    |
| Poisson's ratio                        | 0.34  | 0.33  |
| A, MPa                                 | 90    | 148   |
| B, MPa                                 | 292   | 345   |
| N                                      | 0.31  | 0.183 |
| C                                      | 0.025 | 0.001 |
| M                                      | 1.09  | 0.859 |
| $T_m$ , °C                             | 1083  | 620   |
| $T_{room}$ , °C                        | 25    | 25    |
| Reference strain rate, s <sup>-1</sup> | 1     | 1     |

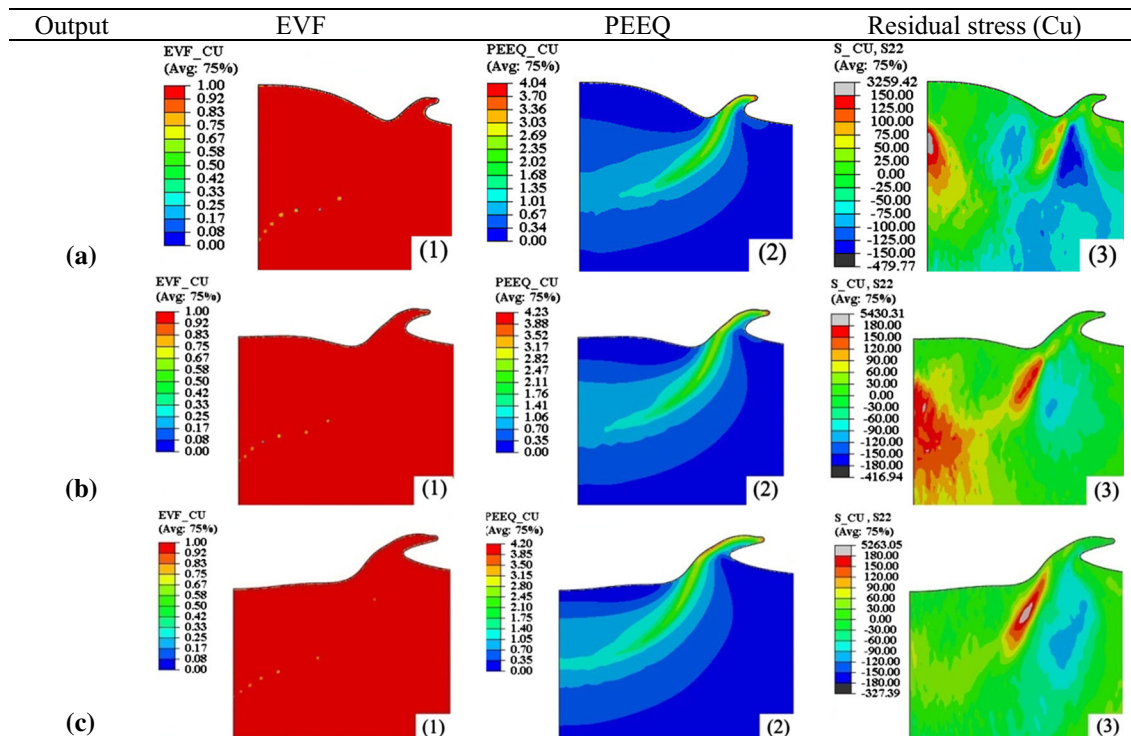


**Fig. 3** The simulation results of (1) the void material volume fraction in elements (EVF), (2) effective plastic strain (PEEQ), and (3) residual stress (S22) in a single splat Cu on Cu at 25 °C with the particle velocity: (a) 500 m/s, (b) 600 m/s, and (c) 700 m/s

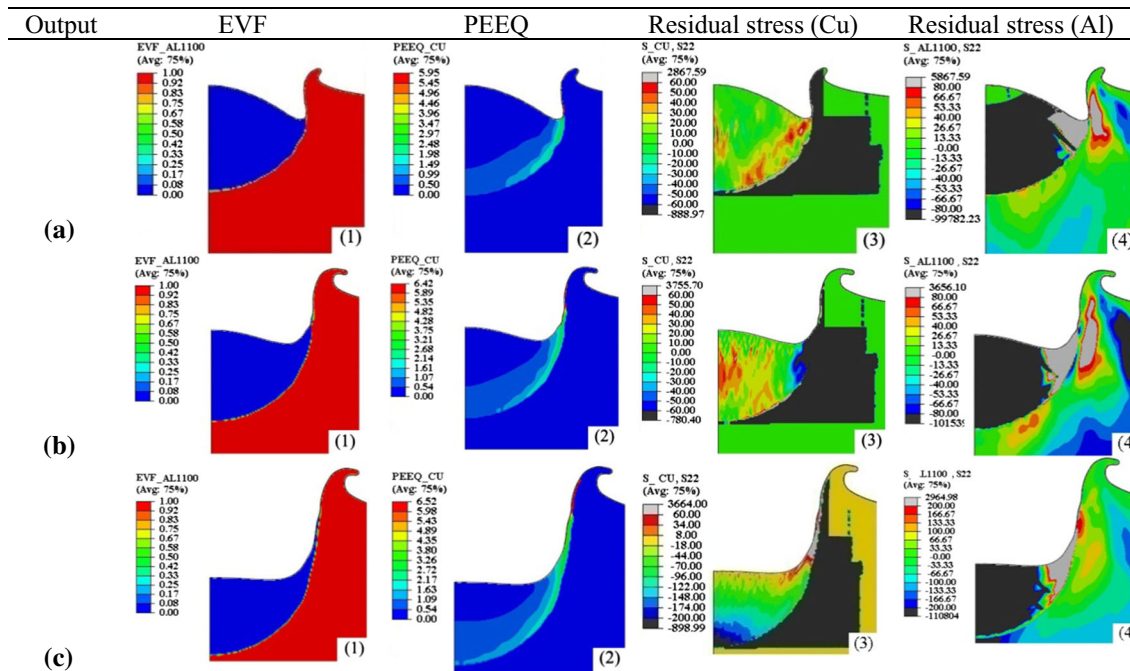


**Fig. 4** The simulation results of (1) the EVF, (2) PEEQ, (3) residual stress of Cu particle, and (4) residual stress of Al substrate in a single splat Cu on Al at 25 °C with the particle velocity: (a) 500 m/s, (b) 600 m/s, and (c) 700 m/s

to 700 m/s because of the increasing kinetic energy. From the simulation results (Fig. 3), it is argued that with the increase of impacting velocity, the residual tensile stress increases. In a previous study (Ref 15), it was found that the residual stress was all compressive in cold-sprayed Cu splats. It was argued that the residual stress value was dependent on the elasto-plastic properties of the particle and the substrate, rather than spraying parameters like velocity. Comparing current simulation results with the previous study (Ref 15), it is proposed that tensile stress exists in most of the material near the Cu/Cu interface and compressive stress exists in a very small part. And this is different from the conclusion of others although the magnitudes of the residual stress in both investigations are small.

In the simulation of Cu/Al as shown in Fig. 4, it can be seen that the residual stress in the center bottom under lower velocity conditions (500 and 600 m/s) is tensile and it presents a compressive state under higher velocity (700 m/s). It should be noted that there exist two residual stress states under different conditions as mentioned above, and the final residual stress state is the result of the interaction of two factors (1) the deposition stress (DS) and the thermal stress (TS) (Ref 10); (2) the tensile stress caused by the action of friction shear (FTS). The extreme velocities in cold spraying cause plastic deformation of the particles on impact, which in turn creates very dense coatings. An analogy of how a cold spray coating is created is that the particles are essentially friction welded to each other during impact. Hence it is pointed out here that the action of friction shear is one of the essential factors that determine the final residual stress. In this case, the

high density and low CTE of Cu affecting the ratio of peening stress to quenching stress during Cu deposition make the DS present a compressive state (Ref 10). The nature of the thermal stress (tensile, neutral, or compressive) is determined by  $\Delta\text{CTE}$  between the coating and substrate. Because the CTE of Cu ( $16.4 \mu\text{m m}^{-1}\text{C}^{-1}$ ) is lower than Al ( $23 \mu\text{m m}^{-1}\text{C}^{-1}$ ) the TS in Cu particle is compressive (Ref 10). Under lower velocity of 500 and 600 m/s, the absolute value of the compressive stress caused by DS and TS is less than that of FTS indicating that the FTS is predominant, which makes the final residual stress tensile. Conversely, the absolute value of compressive stress is larger than the tensile stress indicating the former is predominant, which makes the final residual stress compressive under high velocity of 700 m/s. In a previous study (Ref 16), it was indicated that a compressive stress was generated inside the single-deformed Al particle for both deformation and peening during impact at a velocity of 600 m/s. The difference between the two studies can be attributed to the different materials and different experimental parameters.

It is noteworthy that the deformation and spreading out of the impacting particle against the substrate cause friction shear of the thin layers adjacent to the surface at the surrounding area. Interaction of these layers near the surface results in the residual tensile stress near the surface at the surrounding area (as shown in Fig. 3 and 4). This result is similar to the previous experiment by the author (Ref 23), as shown in Fig. 5, where the cold-sprayed Cu and Al particle interface presents cracks, which reflects the tensile stress near the interface caused by friction shear resulting in the detachment from the bulk

of the Al particle as indicated by arrow. Because of different hardnesses of Cu and Al, the magnitude of particle residual stress in Cu/Al is obviously lower than that in Cu/Cu case. In addition, according to the reported results (Ref 24), it was argued that the residual stresses were strongly influenced by yield stress. From the above simulation results, it can be concluded that the velocity does have influence on the final residual stress.

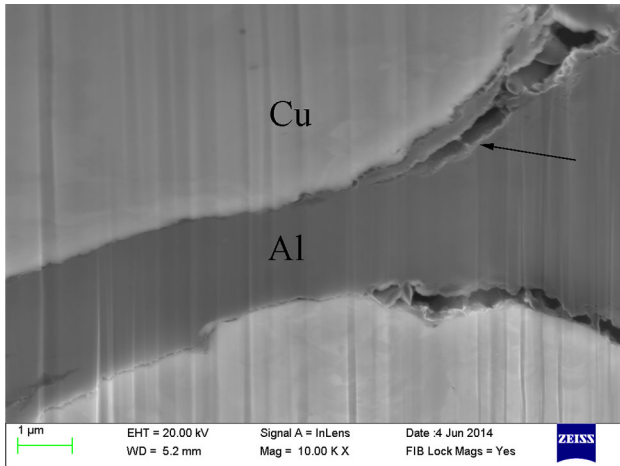


**Fig. 5** The cold-sprayed interface between Cu and Al particles cut by the focused ion beam (FIB) (Ref 20)

**3.1.2 The Influence of Temperature.** The simulation results of the EVF, PEEQ, and residual stresses (including impacting particle and substrate) after impacting at different temperatures (100, 200, and 300 °C) are shown in Fig. 6 and 7. The impact crater becomes deeper with increasing impact temperature and the jet becomes more evident, and the magnitude of particle residual stress in Cu/Cu is obviously higher than that in Cu/Al, which is consistent with results in section 3.1.1. From the simulation results of Cu/Cu, it can be seen that large residual tensile stress exists at the interface. Although the influence of temperature is not very obvious, the residual stress first increases and then decreases with increasing the temperature. Figure 6(a3-c3) also shows the residual stress in Cu substrate, the residual compressive stress at the surrounding of contact interface first increases and then decreases with increasing the temperature. From the simulation results of Cu/Al, the residual stress at the edge of the impact particle changes from compressive to tensile with the increase in particle temperature. Increasing the temperature, causes the impact particle to deform more extensively. Meanwhile, the stress (including tensile stress and compressive stress) of each part increases, while the FTS becomes more predominant, which causes the final residual stress to change from compressive to tensile. Figure 7(a4-c4) shows the residual stress in an Al substrate, and it can be seen that the residual tensile stress near the interface decreases with increasing the temperature.

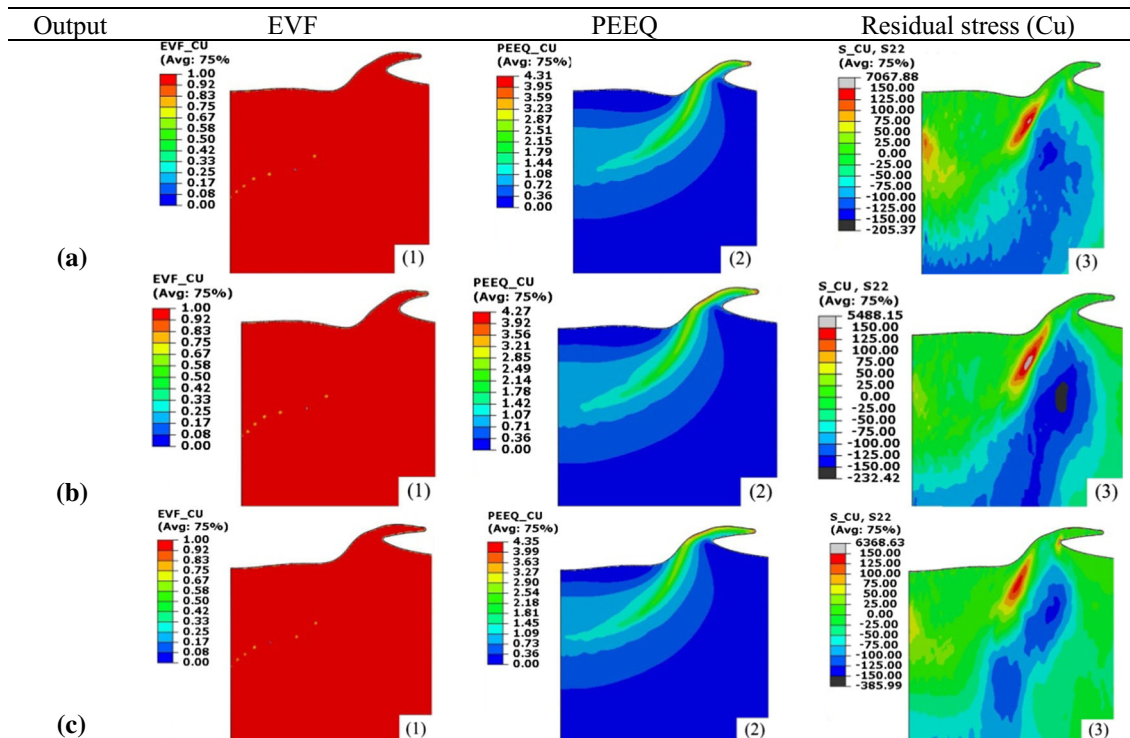


**Fig. 6** The simulation results of (1) the EVF, (2) PEEQ, and (3) residual stress of Cu in single splat Cu on Cu at 600 m/s with the temperature: (a) 100 °C, (b) 200 °C, and (c) 300 °C

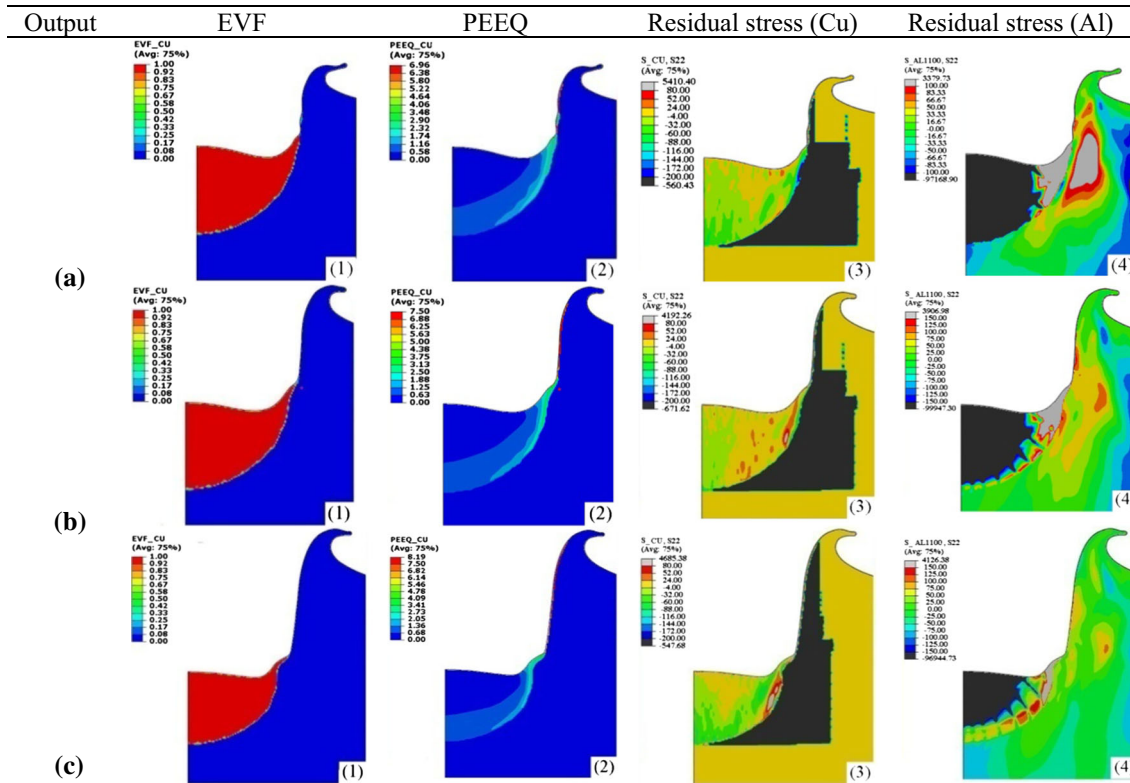
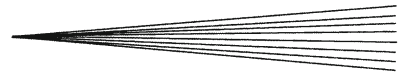


**Fig. 7** The simulation results of (1) the EVF, (2) PEEQ, (3) residual stress of Cu particle, and (4) residual stress of Al substrate in single splat Cu on Al at 600 m/s with the temperature: (a) 100 °C, (b) 200 °C, and (c) 300 °C

In the previous study (Ref 15), it was pointed out that the in-flight particle temperature has negligible effect on the residual stress. Combining with the findings of this paper, it is argued that the influence of temperature on the residual stress is much related to the material combination. The influence is very little in Cu/Cu material system, while there exists a large influence in Cu/Al material system.

Because of the nature of cold spraying, mainly compressive stresses are expected, however, tensile stresses are also found in the simulation of single splat, which is consistent with the previous study (Ref 10). The state of residual stress may vary significantly, depending on the material combination, particle velocity, and temperature.

### 3.2 Residual Stress in Single Pass Coating

Figure 8 and 9 show the simulation results of the PEEQ and residual stress in single pass Cu coating on Cu and Al substrates with the velocities of 300, 500, 600, and 700 m/s. The values greater than zero (from light-green to red and light-gray) are tensile, while the values less than zero (from green to blue and dark-gray) are compressive. It can be clearly seen that there are residual compressive stress and residual tensile stress inside the Cu coating and they non-uniformly distribute to maintain the balance of force. Figure 10 shows the through-thickness stress distributions of Cu/Cu and Cu/Al, and it

can be found from Fig. 10(a) that the residual tensile stress in a Cu substrate increases with increasing the particle velocity. This finding is different from the reported experimental results (Ref 5, 10). Figure 11 shows the reported results in Ref 5, in which it was argued that compressive stress exists in most part of the coating and it was treated as layered distribution similar to the residual stress distribution in thermal sprayed coatings. In Ref 10, it was considered that the DS and TS in Cu coating on Al substrate are both compressive stress, and it makes the final residual stress in Cu coating compressive. In the present work, the large stresses in both cases are concentrated at the inter-particle interfaces inside the coating and this phenomenon is the same with the single splat (section 3.1). And the representative residual stress distribution in the X-direction at the surface layer of the coating is shown in Fig. 12, indicating that the residual stress at the substrate surface also changes greatly. The interfacial residual stress between the coating and substrate can be compressive or tensile.

For single pass Cu/Cu, at a low velocity range of 300-500 m/s, the maximum residual compressive and tensile stresses increase with increasing impact velocity, making the residual stress distribution range wider. After reaching a velocity between 500 and 700 m/s, the value of the residual stress does not change very much with increasing the impact velocity.

In single pass Cu/Al, similar to the Cu/Cu case, at a low velocity range of 300-500 m/s, the residual stresses increase with increasing impact velocity. After reaching a certain velocity between 500 and 700 m/s, the influence of the velocity is not as large as that at low velocity range, and the residual compressive stress increases slowly with the increase of velocity. There are some investigations on the effect of particle velocity in the previous papers (Ref 5, 16, 24) which are consistent with the simulation results in the present study. In Ref 5, 24, the residual stress increased with an increase in the velocity in pure Al coating. And in Ref 16,

**Fig. 9** The simulation results of (1) the EVF, (2) PEEQ, (3) residual stress of Cu particle, and (4) residual stress of Al substrate in single pass Cu on Al at 20 °C with the particle velocity: (a) 300 m/s, (b) 500 m/s, (c) 600 m/s, and (d) 700 m/s

it was indicated that the residual stress changed very little within velocities of 620-765 m/s. A table has been made to make the residual stress variation trend clearer (Table 2). In addition, in the Cu/Cu coating, the nominal value of the residual stress at the velocity of 300 m/s is about -60 MPa, and the values at the velocities of 500, 600, and 700 m/s are about -80 MPa, which are to some extent comparable to

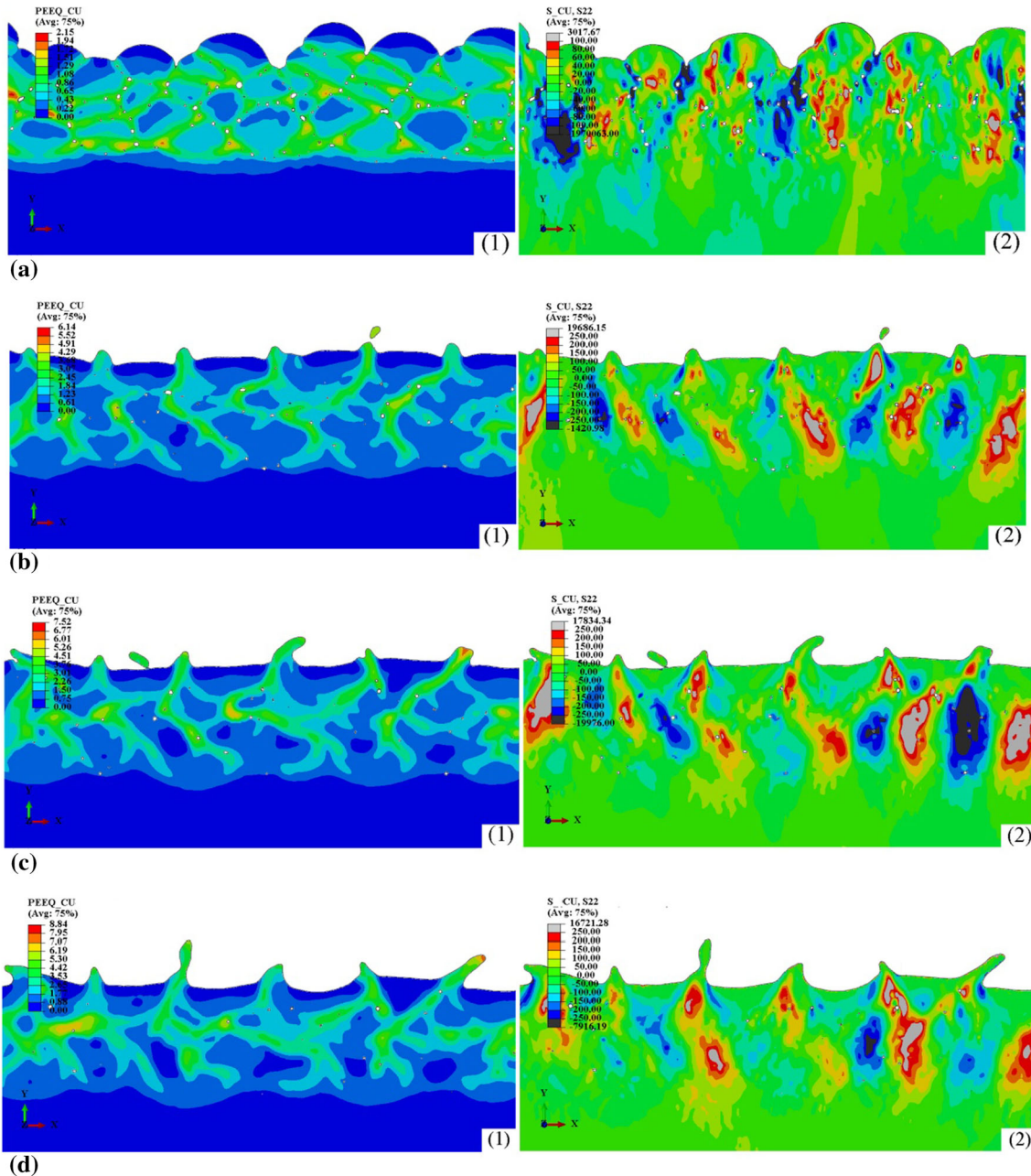
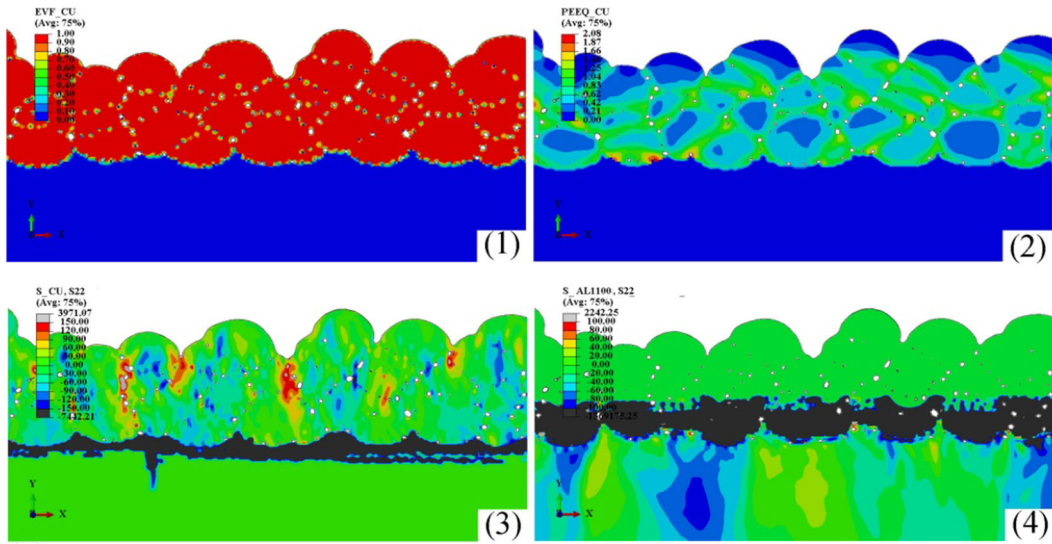
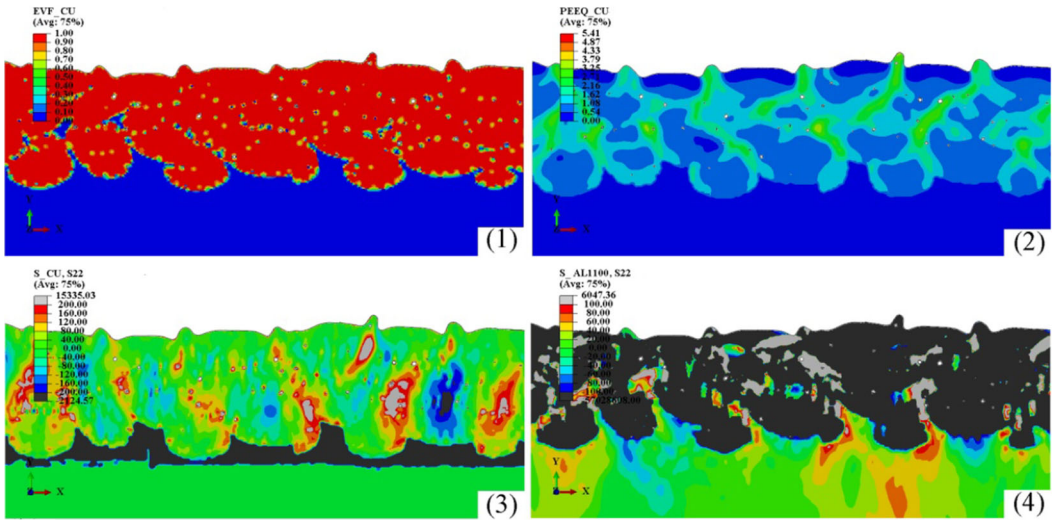


**Fig. 8** The simulation results of (1) the PEEQ and (2) residual stress in single pass Cu on Cu at 25 °C with the particle velocity: (a) 300 m/s, (b) 500 m/s, (c) 600 m/s, and (d) 700 m/s

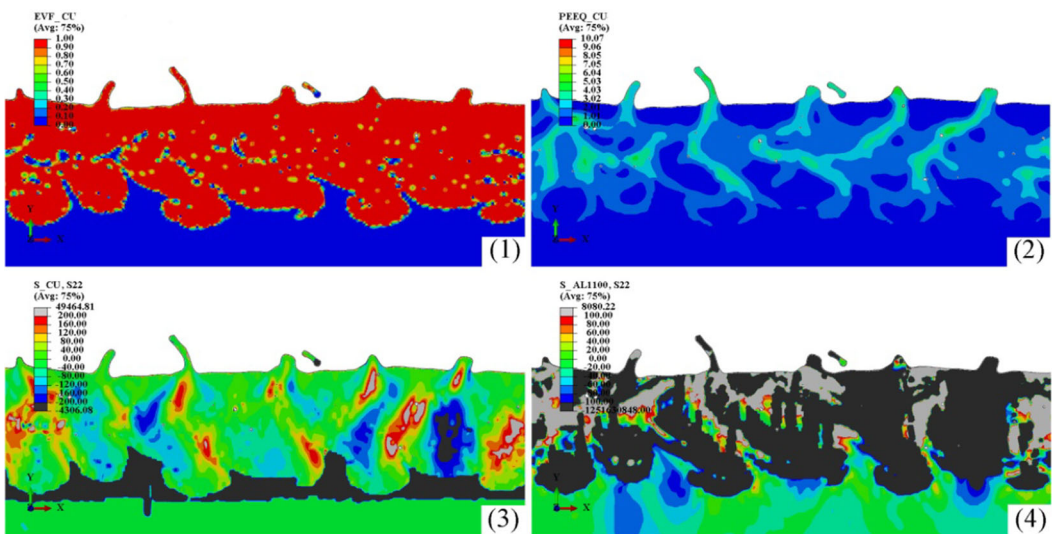




(a)



(b)



(c)

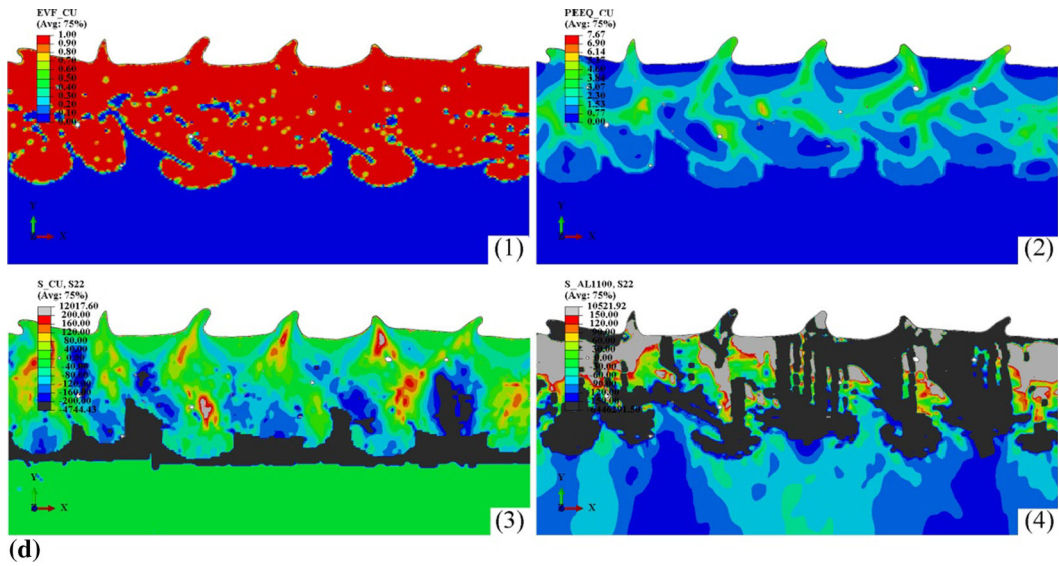
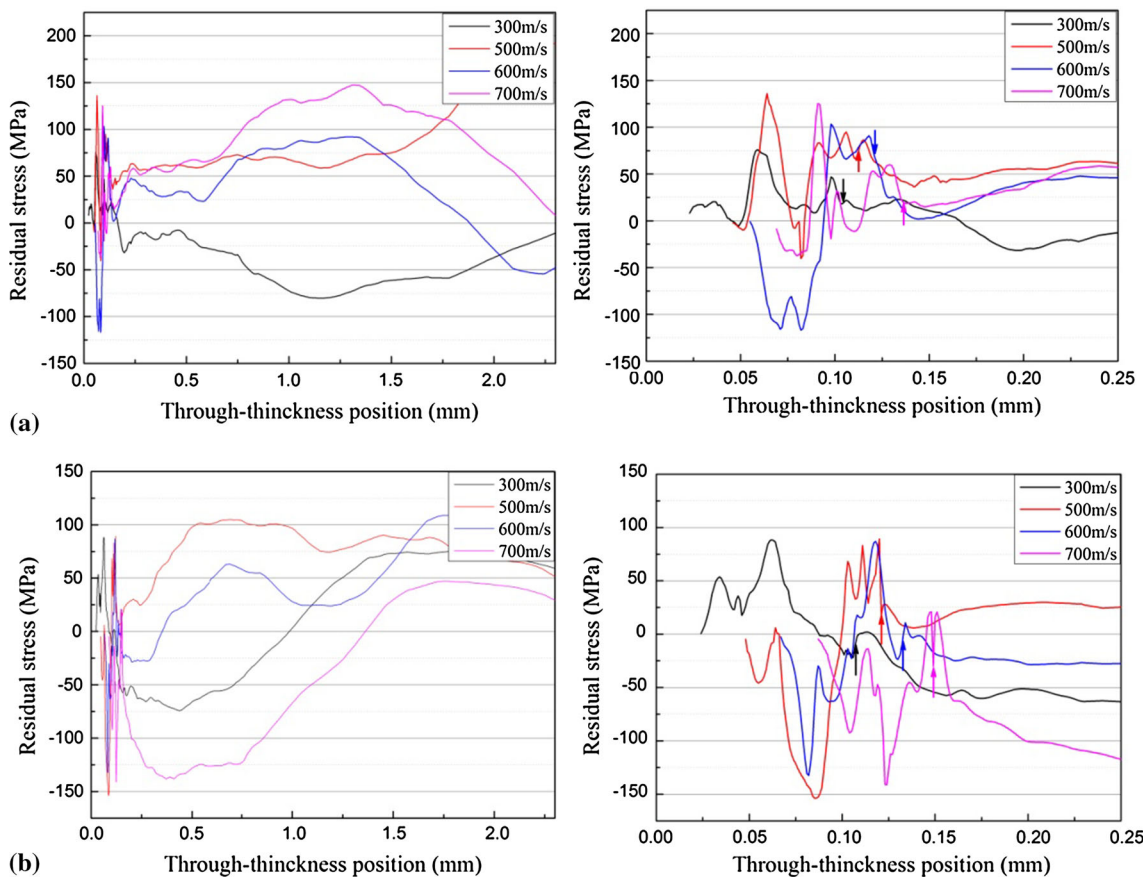
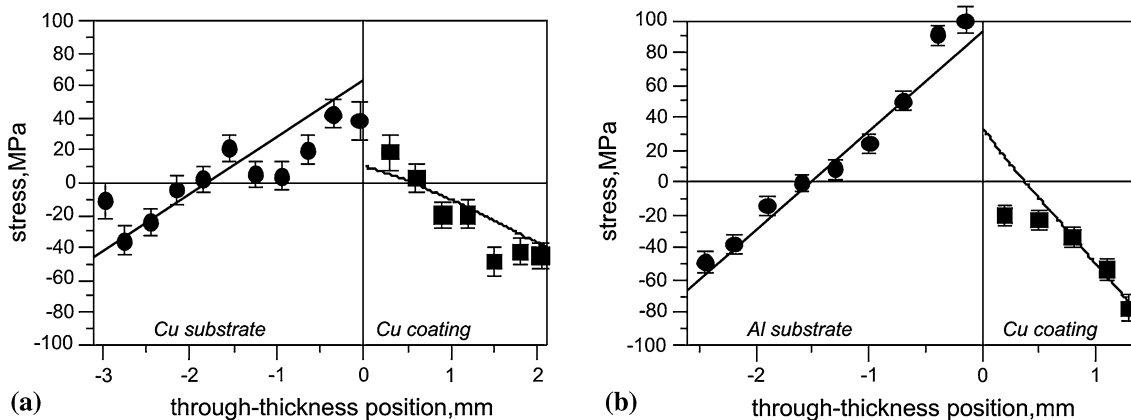


Fig. 9 continued



**Fig. 10** The through-thickness residual stress distributions for (a) Cu on Cu and (b) Cu on Al. The right picture for each figure is the enlarged view near the coating/substrate interface. The interfaces between the coating and substrate are marked by arrows (Color figure online)



**Fig. 11** The experimental results reported by Luzin et al. (Ref 5)

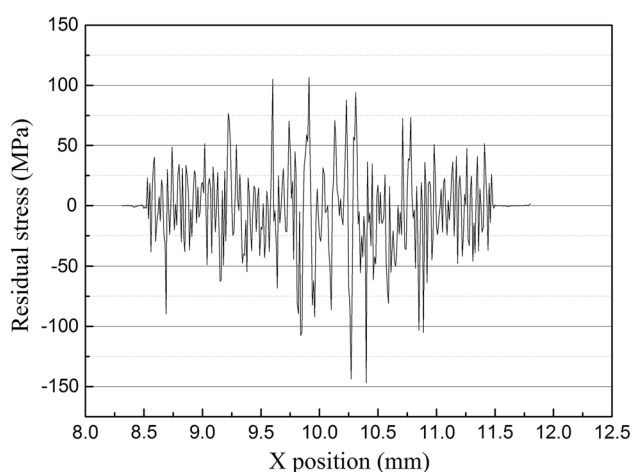


**Fig. 12** The residual stress distribution in the  $X$ -direction at the substrate surface

**Table 2** The residual stress variation trend

| Velocity                   | 300-500 m/s  | 500-700 m/s  |
|----------------------------|--|--|
| Cu/Cu material combination | Residual stresses increase with increasing impact velocity | Value of residual stress does not change very much with increasing the impact velocity |
| Cu/Al material combination | Residual stresses increase with increasing impact velocity | Residual compressive stress increases slowly with the increase of velocity             |

the reported nominal values of cold-sprayed Cu coating, such as  $-60$  MPa (Ref 4) and  $-84$  MPa (Ref 5).

## 4. Conclusions

The residual stress profiles have been simulated for cold-sprayed single Cu splat and single pass Cu coating on

Cu or Al substrates. The influences of particle impact velocity, temperature, and material combination have been investigated. The conclusions are drawn as follows:

- (i) For single Cu splat, in general, the maximum residual stress and plastic deformation are concentrated at the surrounding of the contact zone rather than at the center point of initial impact. The residual stress is the resultant from the combined effects of DS, TS, and FTS. It is worth noting that large tensile stress in the particle and compressive stress in the substrate exist near the interface, which may cause cracks. The impact velocity does have influence on the final residual stress whether Cu/Cu or Cu/Al. The influence of temperature on the residual stress is dependent on the material system and a large influence exists in Cu/Al material system. Compressive and tensile stresses are all found in the simulation of single Cu splat, indicating that the state of residual stress can vary significantly, depending on the material system, particle velocity, and temperature.
- (ii) For single pass Cu coating, the residual stress can vary throughout the coating and not only compressive stress but also tensile stress exists to maintain the balance of force. At low impact velocities of 300-500 m/s, the maximum residual compressive and tensile stresses increase with the increase of velocity. After reaching certain velocity between 500 and 700 m/s, the value of the residual stress does not change very much with increasing velocity in Cu/Cu material combination, while that changes slightly with the increase of velocity in Cu/Al material combination. The simulated stresses are to some extent comparable to the reported experimental values.

## Acknowledgments

This work is supported by the State Key Lab of Advanced Metals and Materials (2013-ZD07), the Fun-

damental Research Funds for the Central Universities (3102014JC02010404), and the 111 Project (B08040).

## References

1. A. Papyrin, Cold Spray Technology, *Adv. Mater. Proc.*, 2001, **9**(159), p 35-51
2. H. Assadi, F. Gartner, T. Stoltenhoff, and H. Kreye, Bonding Mechanism in Cold Gas Spraying, *Acta Mater.*, 2003, **51**, p 4379-4394
3. R. Ghelichi, D. MacDonald, S. Bagherifard, H. Jahed, M. Guagliano, and B. Jodoin, Microstructure and Fatigue Behavior of Cold Spray Coated Al5052, *Acta Mater.*, 2012, **60**(19), p 6555-6561
4. Z. Arabgol, H. Assadi, T. Schmidt, F. Gartner, and T. Klassen, Analysis of Thermal History and Residual Stress in Cold-Sprayed Coatings, *J. Therm. Spray Technol.*, 2013, **23**(1-2), p 84-90
5. V. Luzin, K. Spencer, and M.X. Zhang, Residual Stress and Thermo-Mechanical Properties of Cold Spray Metal Coatings, *Acta Mater.*, 2011, **59**(3), p 1259-1270
6. R. Ghelichi, S. Bagherifard, D. MacDonald, and I. Fernandez-Pariente, Experimental and Numerical Study Residual Stress Evolution in Cold Spray Coating, *Appl. Surf. Sci.*, 2014, **288**(1), p 26-33
7. P. Bansal, P.H. Shipway, and S.B. Leen, Residual Stresses in High-Velocity Oxy-Fuel Thermally Sprayed Coatings-Modelling the Effect of Particle Velocity and Temperature During the Spraying Process, *Acta Mater.*, 2007, **55**(15), p 5089-5101
8. W.B. Choi, L. Li, V. Luzin, R. Neiser, T. Gnaupel-Herold, H.J. Prask, S. Sampath, and A. Gouldstone, Integrated Characterization of Cold Sprayed Aluminum Coatings, *Acta Mater.*, 2007, **55**(3), p 857-866
9. S. Sampath, X.Y. Jiang, J. Matejcek, L. Prchlik, A. Kulkarni, and A. Vaidya, Role of Thermal Spray Processing Method on the Microstructure, Residual Stress and Properties of Coatings: An Integrated Study for Ni-5 wt.%Al Bond Coats, *Mater. Sci. Eng. A*, 2004, **364**(1-2), p 216-231
10. T. Suhonen, T. Varis, S. Dosta, M. Torrell, and J.M. Guilemany, Residual Stress Development in Cold Sprayed Al, Cu and Ti Coatings, *Acta Mater.*, 2013, **61**(17), p 6329-6337
11. A.S.M. Ang and C.C. Berndt, A Review of Testing Methods for Thermal Spray Coatings, *Int. Mater. Rev.*, 2014, **59**(4), p 179-223
12. J. Matejcek and S. Sampath, In Situ Measurement of Residual Stresses and Elastic Moduli in Thermal Sprayed Coatings: Part 1: Apparatus and Analysis, *Acta Mater.*, 2003, **51**(3), p 863-872
13. Y.C. Tsui and T.W. Clyne, An Analytical Model for Predicting Residual Stresses in Progressively Deposited Coatings Part 1: Planar Geometry, *Thin Solid Films*, 1997, **306**, p 23
14. A. Brenner and S. Senderoff, A Spiral Contractometer for Measuring Stress in Electrodeposits, *J. Res. Natl. Bur. Stand.*, 1949, **42**, p 105
15. J. Matejcek and S. Sampath, Intrinsic Residual Stresses in Single Splat Produced by Thermal Spray Processes, *Acta Mater.*, 2001, **49**(11), p 1993-1999
16. S. Rech, A. Trentin, S. Vezzù, J.G. Legoux, E. Irissou, and M. Guagliano, Influence of Pre-Heated Al 6061 Substrate Temperature on the Residual Stresses of Multipass Al Coatings Deposited by Cold Spray, *J. Therm. Spray Technol.*, 2010, **20**(1-2), p 243-251
17. W.Y. Li, H.L. Liao, C.J. Li, H.S. Bang, and C. Coddet, Numerical Simulation of Deformation Behavior of Al Particles Impacting on Al Substrate and Effect of Surface Oxide Films on Interfacial Bonding in Cold Spraying, *Appl. Surf. Sci.*, 2007, **253**(11), p 5084-5091
18. M. Yu, W.Y. Li, F.F. Wang, and H.L. Liao, Finite Element Simulation of Impacting Behavior of Particles in Cold Spraying by Eulerian Approach, *J. Therm. Spray Technol.*, 2011, **21**(3-4), p 745-752
19. C.J. Li, W.Y. Li, and H. Liao, Examination of the Critical Velocity for Deposition of Particles in Cold Spraying, *J. Therm. Spray Technol.*, 2006, **15**, p 212-222
20. G.R. Johnson and W.H. Cook, Fracture Characteristics of Three Metals Subjected to Various Strains, Strain Rates, Temperatures and Pressures, *Eng. Fract. Mech.*, 1985, **21**(1), p 31-48
21. Abaqus Analysis User's Manual, ABAQUS 6.13 HTML Documentation, Dassault Systèmes, 2013
22. D.J. Benson and S. Okazawa, Contact in a Multi-Material Eulerian Finite Formation, *Comput. Methods Appl. Mech. Eng.*, 2004, **193**(39-41), p 4277-4298
23. W.Y. Li, K. Yang, and D.D. Zhang, Interface Behavior of Particles Upon Impacting during Cold Spraying of Cu/Ni/Al Mixture, *6<sup>th</sup> Asian Thermal Spray Conference*, Hyderabad India, 2014, p 33-34
24. K. Spencer, V. Luzin, N. Matthews, and M.X. Zhang, Residual stresses in cold spray Al coatings: The effect of alloying and of process parameters, *Surf. Coat. Technol.*, 2012, **206**(19-20), p 4249-4255